Conformations of Primary Amphipathic Carrier Peptides in Membrane Mimicking Environments†

Laurent Chaloin,‡ Pierre Vidal,‡ Annie Heitz,§ Nicole Van Mau,‡ Jean Méry,‡ Gilles Divita,‡ and Frédéric Heitz*,‡

CRBM-CNRS (ERS 0155), Route de Mende, BP 5051, F. 34033 Montpellier Cedex, France, and CBS-CNRS (UMR 9955) and INSERM U 414, Faculté de Pharmacie, 15, Avenue Charles Flahault, F. 34060 Montpellier Cedex, France

Received April 11, 1997; Revised Manuscript Received June 11, 1997⊗

ABSTRACT: Two peptides designed for drug delivery were generated by the combination of a signal peptide with a nuclear localization sequence and are shown to facilitate the cellular internalization of small molecules which are covalently linked to these peptides. In order to understand the mechanism of internalization, the conformations of the peptides were investigated through different approaches both in solution and in membrane-mimicking environments. These peptides are highly versatile and adopt different conformational states depending on their environment. While in a disordered form in water, they adopt an α-helical structure in TFE and in the presence of micelles of SDS or DPC. The structured domain encompasses the hydrophobic part of the peptides, whereas the charged C-termini remain unstructured. In contrast, in the presence of lipids and whatever the nature of the phosphate headgroup, the two peptides mainly adopt an antiparallel β-sheet form and embed in the lipidic cores. This result suggests that the β-sheet is responsible for the translocation through the cellular membranes but also questions the conformational state of signal peptides when associated to hydrophilic sequences.

The cellular uptake of pharmacological agents still requires considerable improvements especially with respect to the penetration efficiency of the drug and its target selectivity. The cell nucleus is one of the privileged targets since it is involved in the transfer of biological information and in the regulation of cell proliferation. It is therefore of major importance to facilitate access to the nucleus of drugs without having to use "monocellular" techniques, such as microinjection or techniques which are restricted to a small number of cells as it is the case for electroporation *(1*−*4)*. For this purpose and focusing on the improvement of the cell delivery efficiency *(5*−*7)*, we have designed a series of peptides consisting of a hydrophobic sequence, namely the signal peptide sequence of *caïman crocodylus* Ig(v) light chain *(8)*, associated with the nuclear localization sequence (NLS)[1] of the SV40 large T antigen *(9*−*11)*, the two being separated or not by a linker sequence which was thought to be protease sensitive *(12)*. The role of each sequence is, respectively, to facilitate anchoring to the membrane and to enhance intracellular nuclear addressing. Both were selected mainly on the basis of criteria arising from the peptide synthesis strategy (lack of numerous Arg residues and of bulky alkyl side chains such as Val). The two peptides thus designed have the following sequences: Ac-Met-Gly-Leu-Gly-Leu-His-Leu-Leu-Val-Leu[10]-Ala-Ala-Ala-Leu-Gln-Gly-Ala-Trp-Ser-Gln[20]-Pro-Lys-Lys-Lys-Arg-Lys-Val-Cya and Ac-Met-Gly-Leu-Gly-Leu-His-Leu-Leu-Val-Leu[10]-Ala-Ala-Ala-Leu-Gln-Gly-Ala-Lys-Lys-Lys[20]-Arg-Lys-Val-Cya, where Ac is an N-terminal acetyl group and Cya a cysteamide (-NH-CH_2-CH_2-SH) group *(13, 14)*. The cysteamide function was introduced at the C-terminus of each peptide since it is compatible with the solid phase synthetic procedure and allows postsynthetic modifications of the peptides, i.e., covalent linking of a biological active drug or of a fluorescent probe which enables the detection of the cellular localization(s) of the peptides. These two peptides are designated hereafter as **1** and **2**, respectively. In these two peptides the 16 N-terminal residues correspond to the signal peptide while the seven C-terminal ones of peptide **1** correspond to the NLS.

In this paper, we show that the peptides can enter fibroblasts very rapidly and localize mainly to the nucleus. This work is also concerned with a conformational study of the peptides in various media, in particular in media considered as mimicking a membrane environment, and describes the conformational behavior of the two peptides both in solution in water or organic solvents and when incorporated into various types of micelles or in lipid vesicles as investigated by CD, FTIR, fluorescence, ^{1}H NMR, and surface tension measurements on mixed monolayers at the air/water interface. These peptides adopt different but well-defined conformations depending on the nature of medium.

MATERIALS AND METHODS

Materials. The peptides have the same origin as described by Chaloin *et al. (12)*. They were synthesized by solid phase

† This work was supported by the GDR "Peptides et Protéines Amphipathiques" from the CNRS. LC was supported by a grant from the ANRS.

* Address correspondence to CRBM-CNRS, Route de Mende, 34033 Montpellier Cedex, France. Tel: 33 (0)4 67 61 33 92. Fax: 33 (0)4 67 52 15 59.E-mail: fheitz@merlin.crbm.cnrs-mop.fr.

‡ CRBM-CNRS.

§ CBS-CNRS and INSERM u 414.

⊗ Abstract published in *Advance ACS Abstracts,* September 1, 1997.

[1] Abbreviations: NLS, nuclear localization sequence; Cya, cysteamide; UV, ultraviolet; CD, circular dichroism; FTIR, Fourier transform infrared; NMR, nuclear magnetic resonance; AEDI, aminiethyldithio 2-isobutyric acid; HPLC, high-performance liquid chromatography; DOPC, dioleoylphophatidylcholine; DOPS, dioleoylphosphatidylserine; DOPG, dioleoylphosphatidylglycerol; TFE, trifluoroethanol; TFE-d_3, [$^2H_3$]trifluoroethanol, SDS, sodium dodecyl sulfate, SDS-d_{25},[$^2H_{25}$]-sodium dodecyl sulfate; DPC, dodecylphosphocholine; ATR, attenuated total reflectance; 1D, one dimensional; 2D, two dimensional; DQF-COSY, double quantum filtered correlation spectroscopy; TOCSY, 2D total correlation spectroscopy; ROESY, 2D nuclear Overhauser enhancement spectroscopy in the rotating frame; NOESY, 2D nuclear Overhauser enhancement spectroscopy; NOE, nuclear Overhauser enhancement.

S0006-2960(97)00849-0 CCC: $14.00

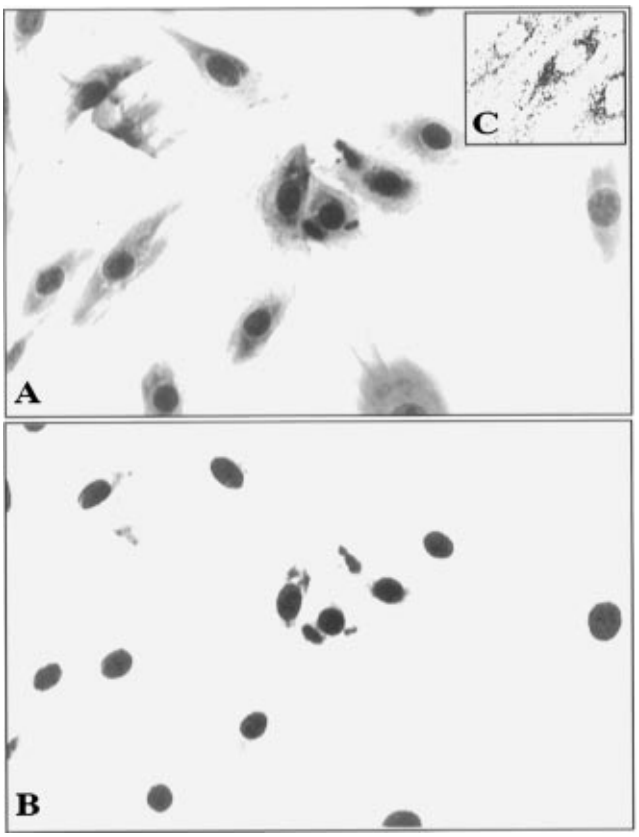

FIGURE 1: Visualization of the localization of the lucifer yellow fluorophore in mammalian fibroblasts: free form and linked to peptide (**1**) Human fibroblasts (Hs-68) were cultured in Dulbecco's modified Eagle's medium supplemented with 8% fetal calf serum. The cells were plated on glass coverslips and incubated for 3 min at 37 °C with the peptide dissolved in Hepes (50 mM, pH 7.2) (30 μL at 5 μM) and then fixed with formalin (3.7%) for 5 min. Coverslips were rinsed with water, stained with Hoechst 33258 and mounted in Airvol 205. Cells were observed by confocal scanning laser microscopy. (A) Confocal section showing the cellular localization which is mainly nuclear of peptide **1** as revealed by the fluorescence of lucifer yellow when linked to peptide. (B) The same section as in panel A but revealed by Hoechst 33258 to show the nuclei. (C) Free form of the fluorophore; here the Lucifer Yellow probe exhibits perinuclear localization.

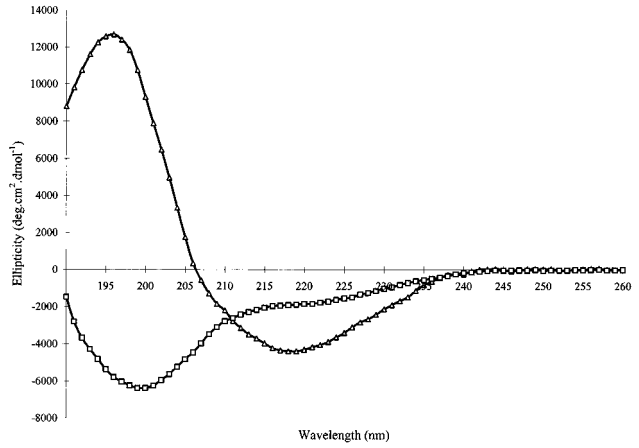

FIGURE 2: Far-UV CD spectrum of peptide **1** in water (25 mM NaCl) (□) and in presence of DOPG vesicles at a molar ratio of 50 (△). Peptide concentration was 5 10^{-5} M and cell path was 1 mm. The ellipticity is given in deg cm^2 dmol^{-1} per peptide unit. Temperature was 25 °C.

peptide synthesis using the Fmoc strategy with AEDI-Expansin resin on a 9050 Pepsynthetizer Milligen (Millipore, U.K.) as reported by Vidal *et al. (15)*. The peptides were purified by semipreparative HPLC with a Nucleosil 300, C8, 5 μm column, 200 × 20, SFCC (Neuilly-Plaisance, France). The N-terminal coumarin-peptide labeling was performed according to the procedure described previously by Vidal et al. *(15)*. They were identified by electrospray mass spectrometry in the positive ion mode using a trio 2000 VG Biotech Mass Spectrometer (Altringham, U.K.) and by amino acid analysis on a High Performance Analyzer (Model 7300, Beckman Instruments, Fullerton, CA).

Table 1: Evaluations of the Amounts of Secondary Structure of Peptides **1** and **2** in Various Media Based on CD and NMR Experiments[a]

	circular dichroism			
peptide **1** (medium)	helix	sheet	random coil	NMR helix
in water	3	28	69	
in 50% TFE	51	0	49	57
with SDS micelles ($R_i = 80$)	43	13	44	53
with DOPG liposomes ($R_i = 80$)	0	72	18	
	circular dichroism			
peptide **2** (medium)	helix	sheet	random coil	NMR helix
in water	10	20	70	
in 50% TFE	42	12	46	
with SDS micelles ($R_i = 80$)	41	14	45	50
with DOPG liposomes ($R_i = 80$)	10	56	34	

[a] The different values were calculated using the Dicroprot software deduced from the CD experiments.

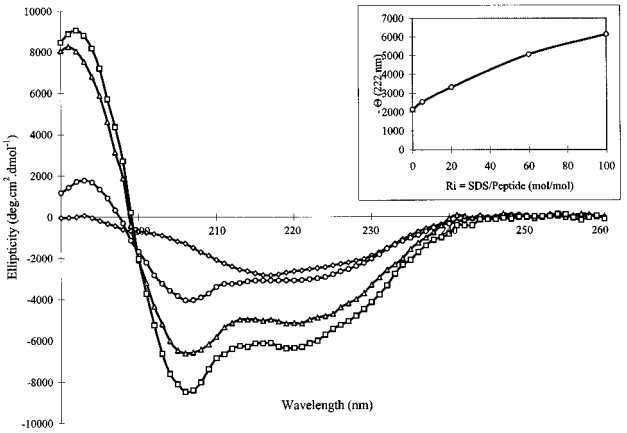

FIGURE 3: Far UV CD spectra of peptide **1** in the presence of micelles of SDS at various SDS/peptide molar ratios (R_i). Peptide concentration was 5 × 10^{-5} M (in water) and cell path was 0.1 mm. (◇) $R_i = 5$, (○) $R_i = 20$, (△) $R_i = 60$, (□) $R_i = 100$. Inset: variation of the ellipticity at 222 nm as a function of R_i.

Chemicals. DOPC, DOPS, DOPG, TFE, and 7-methoxycoumarin-4-acetic acid were purchased from Sigma (St Louis, MO) and SDS, SDS-d_{25}, and TFE-d_3 from Interchim Molecular Probes (Montluçon, France). Dodecylphosphocholine (DPC) was purchased from Avanti Polar Lipids, Inc. (Birmingham, AL).

Cell Culture and Cellular Localization Assays. Human fibroblasts (HS-68) were cultured in Dulbecco's modified Eagle's medium supplemented with 10% foetal calf serum as described previously *(16)*. Cells growing on glass coverslips were incubated for 3 min with lucifer yellow or the peptide coupled to lucifer yellow *(15)* dissolved in Hepes (50 mM, pH 7.2) at a concentration of 5 μM and then fixed with formalin for 5 min. The coverslips were rinsed with water and mounted as described by Girard *et al. (16)*. The localization of the peptides was observed by either confocal laser microscopy or fluorescence microscopy *(17)*.

Preparation of Vesicles. Small unilamellar vesicles (SUVs) were prepared from DOPG or DOPC by sonication.

Table 2: Resonance Assignments for Peptide **1** in SDS-d_{25}/H_2O, pH 3.6, R_i = 100 at 305 K

no.	residue	NH	Hα	Hβ	others
1	Met	8.31	4.42	2.15	γCH_2, 2.65−2.62; SCH_3, 2.15; Ac, 2.15
2	Gly	8.48	4.10−3.99		
3	Leu	8.11	4.29	1.91−1.67	γCH, 1.71; δCH_3, 1.03−0.97
4	Gly	8.48	3.97−3.75		
5	Leu	7.88	4.19	1.76−1.53	γCH, 1.69; δCH_3, 0.97−0.91
6	His	8.17	4.65	3.43−3.34	2H, 8.76; 4H, 7.40
7	Leu	8.27	4.12	2.00−1.62	γCH, 1.91; δCH_3, 1.01−0.94
8	Leu	8.09	4.14	1.95−1.71	γCH, 1.87; δCH_3, 1.02−0.95
9	Val	7.65	3.82	2.35	γCH_3, 1.15−1.06
10	Leu	7.75	4.18	1.90−1.75	γCH, 1.79; δCH_3, 0.99−0.97
11	Ala	8.53	4.01	1.56	
12	Ala	7.95	4.23	1.60	
13	Ala	7.91	4.30	1.64	
14	Leu	8.15	4.24	1.93−1.69	γCH, 1.88; δCH_3, 0.96−0.93
15	Gln	8.08	4.02	2.26−2.15	γCH_2, 2.55−2.42; ϵNH, 7.33−6.75
16	Gly	8.22	4.00−3.93		
17	Ala	7.98	4.36	1.51	
18	Trp	8.08	4.63	3.43−3.36	1H, 10.01; 2H, 7.30; 4H, 7.58; 5H, 7.07; 6H, 7.16; 7H, 7.51
19	Ser	7.82	4.39	3.94−3.89	
20	Gln	7.60	4.52	2.12−2.00	γCH_2, 2.41; ϵNH_2, 7.50−6.81
21	Pro		4.44	2.34−1.93	γCH_2, 2.07−2.00; δCH_2, 3.74−3.66
22	Lys	8.28	4.32	1.91−1.82	γCH_2, 1.49; δCH_2, 1.71; ϵCH_2, 2.97; ζNH_2, 7.37
23	Lys	8.01	4.35	1.89−1.82	γCH_2, 1.45; δCH_2, 1.74; ϵCH_2, 3.07; ζNH_2, 7.47
24	Lys	8.21	4.35	1.88−1.82	γCH_2, 1.49; δCH_2, 1.72; ϵCH_2, 3.05; ζNH_2, 7.49
25	Arg	8.16	4.49	1.98−1.89	γCH_2, 1.72; δCH_2, 3.23; ϵCH, 7.30
26	Lys	8.25	4.32	1.88−1.82	γCH_2, 1.49; δCH_2, 1.74; ϵCH_2, 3.07; ζCH_2, 7.49
27	Val	7.66	4.16	2.15	γCH_3, 1.00
28	Cya	7.92	3.49−3.40	2.71	

Briefly, dry lipids were dissolved in $CHCl_3$:MeOH (3:1 v/v). The solvent was evaporated under a nitrogen stream and desiccated under high vacuum for at least 3 h to remove the residual solvent. The lipids (at a concentration of 2 mg/mL) were resuspended in buffer by vortex mixing. The resulting lipid dispersion was sonicated (∼20 min at 80% pulse cycle in an ice/water bath) with a probe sonicator. All SUV preparations were equilibrated overnight at 4 °C and used on the next day.

Study at the Air/Water Interface. Surface tension measurements were performed according to the Wilhelmy method using a Prolabo (Paris) tensiometer and recorded to a X-Y Kipp and Zonen (Delft, The Netherlands) recorder, Model BD 91. All measurements were made after injection into the subphase (0.154 M NaCl) of aliquots of aqueous solutions of the peptides. The subphase was then gently stirred with a magnetic stirrer, and measurements were made when the surface tension remained constant.

Spectroscopic Measurements. CD measurements were carried out on a Jobin-Yvon Mark V dichrograph at a scan speed of 20 nm/min using quartz cells with 0.1 or 1 mm path width according to the peptide concentration used (concentration range = 10^{-6}−10^{-4} M). All spectra correspond to an averaging of five separate experiments. All spectra were corrected by the baseline obtained for peptide free preparations. The amounts of the various structures were estimated using the Dicroprot software (V2.3d by G. Deléage, IBCP Lyon, France).

Fluorescence spectra were recorded on a spectrofluorimeter Spex-fluorolog Model 1681 (Jobin-Yvon) at 25 °C with a peptide concentration used of 5×10^{-5} M. The excitation wavelength was 280 nm, and emission spectra were recorded in the 310−400 nm range with a band pass of 4 nm. For coumarin-peptide experiments, no fluorescence transfer was observed and the excitation wavelength was therefore 280 nm and the emission spectra were recorded in the 320−500 nm range.

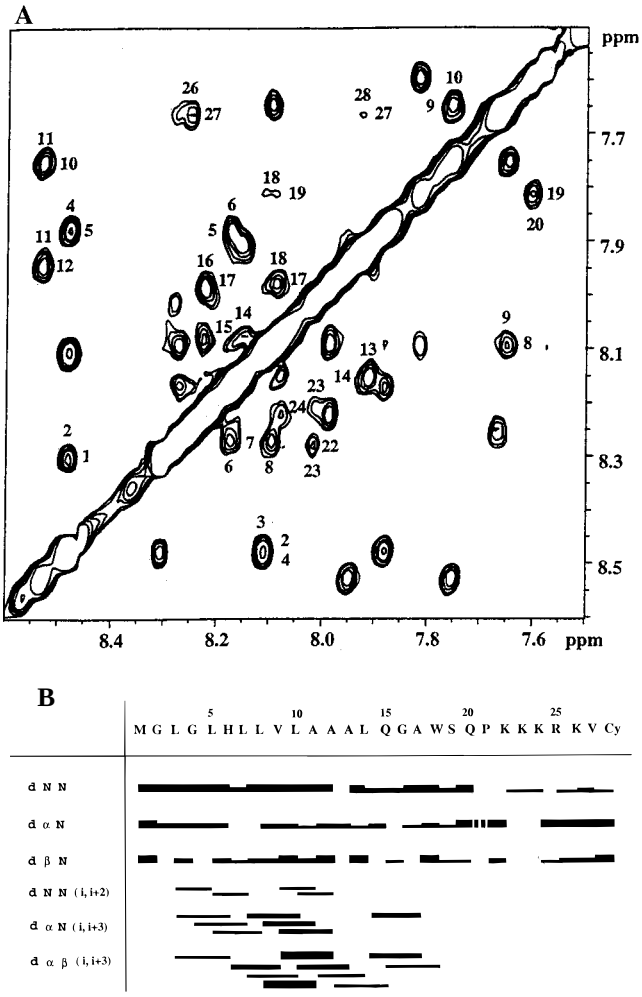

FIGURE 4: (A) N-N region of the NOESY spectrum of peptide **1** (2 mM) in the presence of micelles of SDS-d_{25} at R_i = 100. (B) Medium-range NOE contacts observed in the NOESY spectrum of peptide **1** (2 mM) in SDS-d_{25} at R_i = 100. The thickness of the horizontal bars is indicative of the NOEs relative intensities.

Table 3: Resonance Assignments for Peptide **2** 5.7 mM in H_2O, pH 3.6 at 305 K

no.	residue	NH	Hα	Hβ	others
1	Met	8.42	4.45	2.11−2.04	γCH$_2$, 2.66−2.61; SCH$_3$, 2.13; Ac, 2.08
2	Gly	8.59	3.98		
3	Leu	8.13	4.38	1.64	γCH, 1.72; δCH$_3$, 0.97−0.91
4	Gly	8.47	3.96−3..91		
5	Leu	7.99	4.29	1.63−1.53	γCH, 1.57; δCH$_3$, 0.94−0.89
6	His	8.53	4.70	3.33−3.23	2H, 8.66; 4H, 7.32
7	Leu	8.17	4.31	1.61	γCH, 1.69; δCH$_3$, 0.96−0.90
8	Leu	8.20	4.37	1.64	γCH, 1.72; δCH$_3$, 0.97−0.91
9	Val	8.06	4.06	2.10	γCH$_3$, 0.99−0.96
10	Leu	8.21	4.35	1.68	γCH, 1.63; δCH$_3$, 0.96−0.90
11	Ala	8.22	4.25	1.45	
12	Ala	8.18	4.25	1.45	
13	Ala	8.12	4.30	1.46	
14	Leu	8.02	4.34	1.76−1.71	γCH, 1.68; δCH$_3$, 0.97−0.91
15	Gln	8.18	4.30	2.18−2.07	γCH$_2$, 2.45; εNH$_2$, 7.51−6.89
16	Gly	8.35	3.99−3.95		
17	Ala	8.07	4.32	1.45	
18	Lys	8.20	4.29	1.88−1.81	γCH$_2$, 1.57−1.54; δCH$_2$, 1.72; εCH$_2$, 3.04, ζNH$_2$, 7.56
19	Lys	8.14	4.31	1.86−1.78	γCH$_2$, 1.50−1.45; δCH$_2$, 1.72; εCH$_2$, 3.04; ζNH$_2$, 7.56
20	Lys	8.27	4.32	1.85−1.77	γCH$_2$, 1.50−1.45; δCH$_2$, 1.71; εCH$_2$, 3.04; ζNH$_2$, 7.56
21	Arg	8.33	4.34	1.85−1.78	γCH$_2$, 1.69−1.64; δCH$_2$, 3.24; εNH, 7.21
22	Lys	8.43	4.36	1.84−1.78	γCH$_2$, 1.48−1.42; δCH$_2$, 1.72; εCH$_2$, 3.04; ζNH$_2$, 7.56
23	Val	8.24	4.08	2.07	γCH$_3$, 0.98
24	Cya	8.34	3.45	2.72	

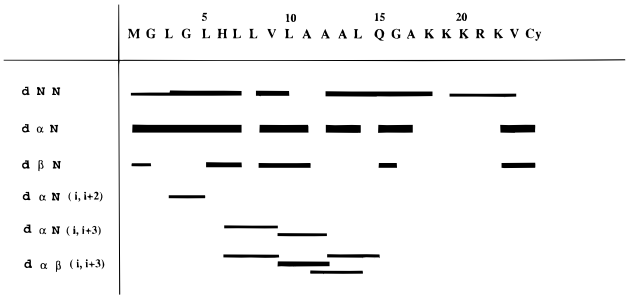

FIGURE 5: Medium-range NOE contacts observed in the NOESY spectrum of peptide **2** (5.7 mM) in water. The thickness of the horizontal bars is indicative of the NOEs relative intensities.

FTIR spectra were obtained on a Bruker IFS 28 spectrometer equipped with a liquid nitrogen cooled MCT detector. The spectra (1000 or 5000 scans) were recorded at a spectral resolution of 4 cm^{-1} on monolayers obtained by spreading solutions in chloroform/methanol (3:1) of mixtures of lipid and peptide onto the water surface, which were transferred onto germanium plates (1 monolayer on each side of the plate). During the transfer, the surface pressure of the monolayer was maintained constant at 30 mN/m through a homemade setup. The Bruker OPUS/IR2 program was used for spectrum analysis. The complex contour observed for the amide I of each peptide was decomposed using second derivative spectroscopy and curve fitting. Band positions for final curve fitting were determined from second derivative spectra. Estimates of the relative contributions of peaks areas to the amide I contour were obtained from the results of curve fitting using the Levenberg−Marquardt algorithm.

NMR experiments were recorded on 400 or 600 MHz Bruker AMX spectrometers. All 2D experiments, DQF-COSY, TOCSY, ROESY, and NOESY, were performed according to the standard procedures *(18)* using quadrature detection in both dimensions with spectral widths of 11.7 ppm in both dimensions. The carrier frequency was centered on the water signal, and the solvent was suppressed by continuous low-power irradiation during the relaxation delay and during the mixing time for NOESY spectra. The 2D spectra were obtained using 2048 or 4096 points for each t1 value and 512 t1 experiments were acquired for TOCSY and ROESY experiments. Increments of 800 t1 were used for DQF-COSY. TOCSY spectra were recorded with spin lock times of 30 and 60 ms. The mixing time was 200 and 300 ms in NOESY spectra and 300 ms in ROESY spectra. Prior to Fourier transform, the time domain data were multiplied by $\pi/8$ and $\pi/4$ phase-shifted sine bell functions for t2 and t1 domains, respectively. NMR studies were performed on 1−6 mM peptide solutions. Peptide **1**, being not soluble enough in pure water to enable NMR measurements, was dissolved in TFE-d_3/H_2O 30:70 and 70:30 (v/v), and the residual signal from protonated TFE was used as a reference at 3.88 ppm *(19)*. Peptide **2** was dissolved in 90% H_2O/D_2O with TSP-d_4 as an internal reference. For the micelle-bound form, 1−2 mM peptide solutions were mixed with 100−200 mM perdeuterated SDS. For **1**, the sample was prepared (2 mM peptide/100 mM SDS-d_{25}) as described by Chupin *et al. (20)*. The pH was adjusted by HCl or NaOH to 3.6−3.7. Most spectra were acquired at 290, 305, and 325 K. Chemical shift assignments of the peptides were achieved by the well-known method developed by Wüthrich *(18)* using TOCSY and DQF-COSY to identify the spin systems and NOESY to connect the adjacent spin systems by sequential NOE.

RESULTS

Since most of the observations made on peptide **1**, the sequence of which is Ac-Met-Gly-Leu-Gly-Leu-His-Leu-Leu-Val-Leu^{10}-Ala-Ala-Ala-Leu-Gln-Gly-Ala-Trp-Ser-Gln^{20}-Pro-Lys-Lys-Lys-Arg-Lys-Val-Cya, were identical to these of peptide **2**, which differs from **1** only by deletion of the Trp-Ser-Gln-Pro sequence, all the results reported here will refer to peptide **1** except when mentioned.

Cellular Localization Assays. Figure 1 shows the cellular localizations of a lucifer yellow probe in human fibroblasts (HS 68) after incubation of the cells in the presence of peptide **1** linked to the probe (panel A) or the free form of the fluorophore (panel C). Clearly, while the free form of the fluorophore did not localize to the nucleus, when linked

Table 4: Resonance Assignments for Peptide **2** in SDS-d_{25}/H_2O, pH 3.6, R_i = 100 at 305 K

no.	residue	NH	Hα	Hβ	others
1	Met	8.30	4.41	2.15	γCH_2, 2.64; SCH_3, 2.15; Ac, 2.15
2	Gly	8.47	4.09−3.99		
3	Leu	8.10	4.29	1.91−1.67	γCH, 1.72; δCH_3, 1.03−0.97
4	Gly	8.47	3.97−3.76		
5	Leu	7.88	4.20	1.74−1.53	γCH, 1.71; δCH_3, 0.96−0.90
6	His	8.18	4.66	3.42−3.33	2H, 8.77; 4H, 7.40
7	Leu	8.24	4.14	2.00−1.63	γCH, 1.90; δCH_3, 1.01−0.94
8	Leu	8.08	4.14	1.94−1.71	γCH, 1.89; δCH_3, 1.01−0.94
9	Val	7.69	3.82	2.33	γCH_3, 1.16−1.06
10	Leu	7.74	4.15	1.90−1.76	γCH, 1.79; δCH_3, 0.98−0.96
11	Ala	8.49	4.02	1.56	
12	Ala	7.96	4.20	1.59	
13	Ala	8.02	4.27	1.62	
14	Leu	8.19	4.19	1.94−1.72	γCH, 1.91; δCH_3, 0.97−0.95
15	Gln	8.15	4.12	2.21	γCH_2, 2.59−2.47; εNH_2, 7.35−6.79
16	Gly	8.28	3.98		
17	Ala	8.04	4.29	1.56	
18	Lys	8.10	4.15	2.02	γCH_2, 1.56; δCH_2, 1.77; εCH_2, 3.08; ζNH_2, 7.54
19	Lys	7.94	4.27	1.93	γCH_2, 1.54; δCH_2, 1.76; εCH_2, 3.06; ζNH_2, 7.52
20	Lys	8.01	4.30	1.94	γCH_2, 1.54; δCH_2, 1.75; εCH_2, 3.05; ζNH_2, 7.49
21	Arg	7.96	4.42	2.01−1.89	γCH_2, 1.75; δCH_2, 3.24; εNH, 7.31
22	Lys	8.16	4.35	1.92−1.89	γCH_2, 1.50−1.47; δCH_2, 1.76; εCH_2, 3.06; ζNH_2, 7.48
23	Val	7.77	4.13	2.16	γCH_3, 1.01
24	Cya	7.96	3.47−3.42	2.72	

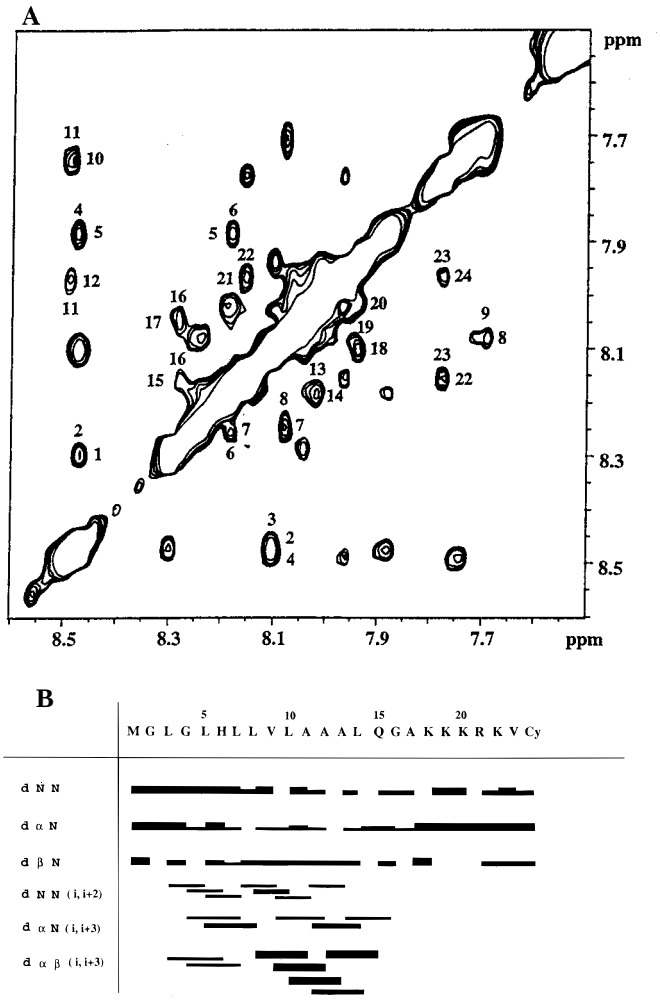

FIGURE 6: (A) N-N region of the NOESY spectrum of peptide **2** (2 mM) in the presence of micelles of SDS-d_{25} at R_i = 100. (B) Medium-range NOE contacts observed in the NOESY spectrum of peptide **2** (2 mM) in SDS-d_{25} at R_i = 100. The thickness of the horizontal bars is indicative of the NOEs relative intensities.

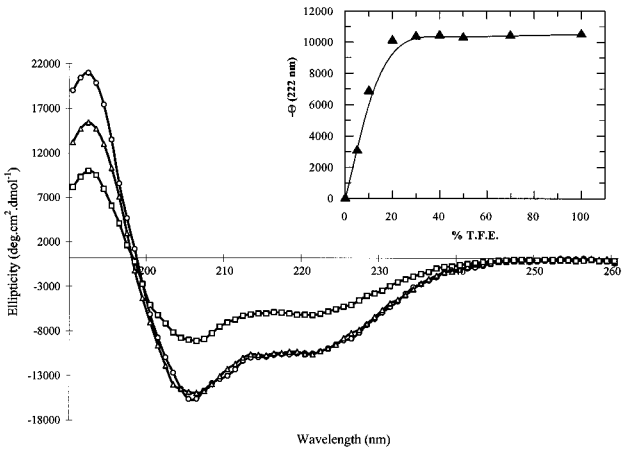

FIGURE 7: Far-UV CD spectra of peptide **1** in water−TFE mixtures of various compositions. (□) 10% TFE (V/V); (△) 20% TFE; (○) 50% TFE. Inset: variation of the ellipticity at 222 nm with the TFE concentration. Peptide concentration: 2×10^{-5} M, cell path 1 mm, 25 °C. The ellipticity is given in deg cm^2 $dmol^{-1}$ per peptide unit.

to the peptide, the final cellular localization of the probe was mainly nuclear after 3 min. incubation. It should be mentioned that although slightly more diffuse, peptide **2** induced a very similar localization (data not shown). Since we could not detect any difference between 4 and 37 °C it is likely that the internalization process does not occur by endocytosis *(21)*. All these observations indicate that peptides **1** and **2** can spontaneously cross the cell membrane. In order to understand the internalization process, we undertook a conformational study of both peptides in various media.

Conformational Studies. When in solution in water, the CD spectra of both peptides are characteristic at low ionic strength (25 mM NaCl) and whatever the pH (3 or 7.2) and the concentration in the 10^{-6}−10^{-4} M range with a single negative extremum at 198 nm (Figure 2), which is usually assigned to a random coil form *(22)* (Table 1). However, when the nature of the environment resembles more membranes such as micelles *(17, 23−25)* or when incorporated into lipid vesicles, the CD spectra of the peptides are strongly modified in a medium-dependent manner.

Since two different types of CD spectra were obtained, one characterizing the presence of α-helical structure, the

Table 5: Resonance Assignments for Peptide **1** 1.5 mM in H_2O/TFE-d_3 (70/30) at 305 K

no.	residue	NH	Hα	Hβ	others
1	Met	8.18	4.26	1.95	γCH_2, 2.54−2.48; SCH_3, 1.98; Ac, 1.98
2	Gly	8.39	3.87		
3	Leu	7.90	4.12	1.61	δCH_3, 0.85
4	Gly	8.23	3.79−3.71		
5	Leu	7.82	4.11	1.58	γCH, 1.53; δCH_3, 0.83−0.77
6	His	7.83	4.16	3.29−3.21	2H, 8.46; 4H, 7.92
7	Leu	7.97	4.06	1.82−1.72	γCH, 1.51; δCH_3, 0.83−0.78
8	Leu	7.75	4.00	1.79	γCH, 1.61; δCH_3, 0.82−0.77
9	Val	7.74	3.58	2.05	γCH_3, 0.95−0.85
10	Leu	7.68	4.02	1.60	γCH, 1.73; δCH_3, 0.78
11	Ala	8.37	3.89	1.41	
12	Ala	8.07	3.98	1.41	
13	Ala	8.27	4.03	1.46	
14	Leu	8.39	3.99	1.72−1.27	γCH, 1.72; δCH_3, 0.75−0.71
15	Gln	7.90	3.98	2.08	γCH_2, 2.41−2.29; ϵNH_2, 7.05−6.50
16	Gly	7.98	3.81		
17	Ala	7.89	4.10	1.24	
18	Trp	7.95	4.56	3.29−3.23	1H, 9.72; 2H, 7.13; 4H, 7.49; 5H, 7.02; 6H, 7.09; 7H, 7.34
19	Ser	7.66	4.31	3.83−3.72	
20	Gln	7.75	4.45	2.05−1.94	γCH_2, 2.36; ϵNH_2, 7.38−6.67
21	Pro		4.34	2.25−1.83	γCH_2, 1.97; δCH_2, 3.74−3.61
22	Lys	8.12	4.18	1.79−1.71	γCH_2, 1.43−1.37; δCH_2, 1.62; ϵCH_2, 2.92; ζNH_2, 7.48
23	Lys	7.90	4.22	1.78−1.70	γCH_2, 1.39−1.33; δCH_2, 1.62; ϵCH_2, 2.92; ζNH_2, 7.48
24	Lys	7.99	4.21	1.77−1.68	γCH_2, 1.39−1.34; δCH_2, 1.62; ϵCH_2, 2.92; ζNH_2, 7.48
25	Arg	7.99	4.26	1.75−1.68	γCH_2, 1.55; δCH_2, 3.10; ϵCH, 7.10
26	Lys	8.16	4.27	1.75−1.68	γCH_2, 1.38−1.32; δCH_2, 1.62; ϵCH_2, 2.92; ζCH_2, 7.48
27	Val	7.80	4.03	1.94	γCH_3, 0.85
28	Cya	7.98	3.55−3.36	2.75	

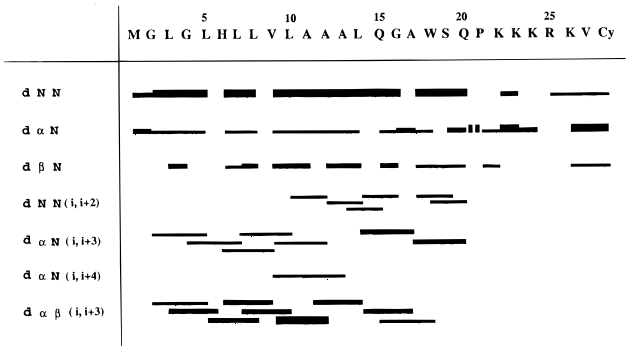

FIGURE 8: Medium-range NOE contacts observed in the NOESY spectrum for peptide **1** (1.5 mM) in a water−TFE-d_3 mixture (70/30 V/V). The thickness of the horizontal bars is indicative of the NOEs relative intensities.

other rather favoring the existence of a β-sheet structure, these two situations were examined in detail separately and are presented below.

(A) Study in Media Inducing the α*-Helical State.* A study carried out in SDS micelles produced CD spectra (Figure 3) which indicate that for both peptides the presence of micelles of SDS induces α-helix structure, characterized by two negative bands at 222 and 207 nm, associated with a positive band at 193 nm. The proportion of α-helix was 43% (Table 1).

The precise localization of the α-helical domain was determined by NMR spectroscopy. For peptide **1**, due to its low solubility in water, it was incorporated into the micelles using the procedure reported by Chupin *et al. (20)* and we first collected 1D spectra as a function of the SDS/peptide ratio (R_i). Since no spectral difference could be detected when R_i was in the range 50−100, the peptide conformation was analyzed in detail at $R_i = 100$ (Table 2) and as usual, determination of secondary structures was provided by the magnitude and the pattern of interresidue NOEs. The various observed dNN(i, $i + 2$), $d_\alpha N(i, i + 3)$,

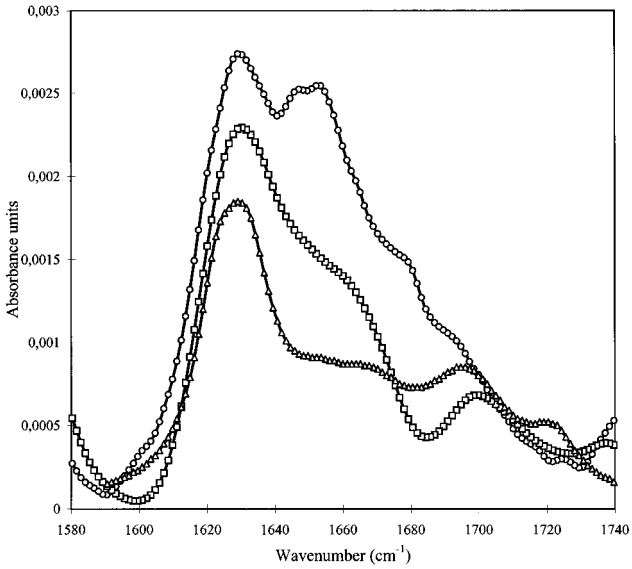

FIGURE 9: FTIR spectrum (amide I region) of a transferred monolayer built of pure peptide **1** (○) and for a peptide/DOPG molar ratio of 1 (△) and using DOPC instead of DOPG (□). The mixtures were dissolved in chloroform/methanol (3:1) before spreading and the transfer was made at a pressure of 30 mN/m onto an ATR germanium plate.

$d_\alpha N(i, i + 4)$, and $d_{\alpha\beta}(i, i + 3)$ NOEs (Figure 4) confirmed the existence of an α-helical conformation extending from residue 3 to residue 18, the remainder of the molecule being disordered. Concerning the water soluble peptide **2**, unfortunately and, as previously noted by Rozek *et al. (26)* for cationic peptides, at low values of R_i (<30), we observed a precipitate thus precluding a study at low R_i. When R_i was increased above 30, the precipitate disappeared and, as already observed for peptide **1**, all spectra between $R_i = 50$ and 100 were identical. When in solution in water (Table 3), this peptide showed only NOEs of the (i, $i + 2$) and (i, $i + 3$) types in the 6−15 region (Figure 5) together with strong sequential $d_\alpha N$, indicating that it only has a tendency

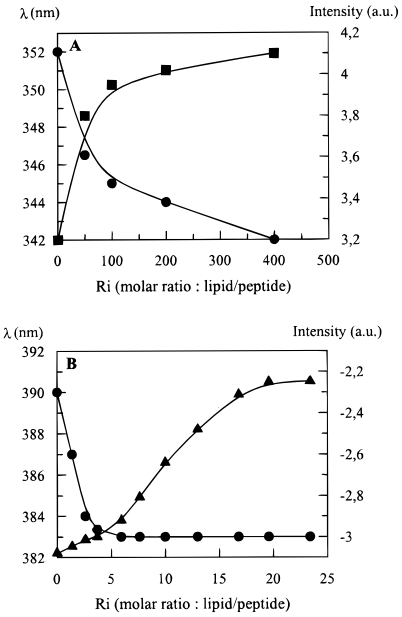

FIGURE 10: Fluorescence experiments of peptide **1** at a concentration of 5×10^{-5} M in sodium phosphate buffer 10 mM, pH 7.2. (A) Tryptophan fluorescence spectra of peptide **1** obtained upon additions of vesicles of DOPG at different R_i. (●) Variation of the maximum wavelength of the tryptophan versus R_i; (■) Variation of the maximum of the tryptophan fluorescence intensity versus R_i. (B) Fluorescence of the coumarin labeled peptide **1** at different values of R_i in DOPG Vesicles. (●) Variation of the maximum wavelength of the coumarin versus R_i; (▲) variation of the maximum of the coumarin fluorescence intensity versus R_i.

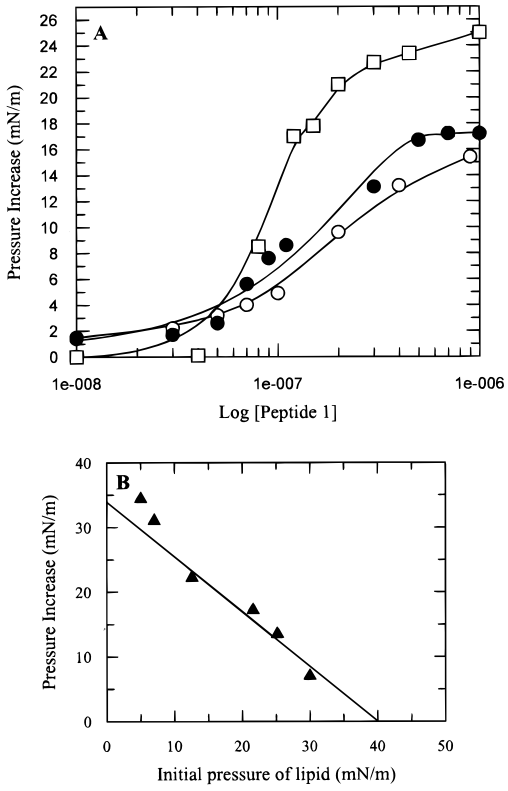

FIGURE 11: Adsorption experiments of peptide **1** at the air−water interface. (A) Relative variations of the surface tensions as a function of the peptide concentration in the subphase; (□) without lipid, (●) in the presence of a DOPG monolayer at an initial pressure 20 mN/m, (○) in the presence of a DOPC monolayer at an initial pressure 20 mN/m. (B) Variation of the maximum pressure increase as a function of the initial pressure of a DOPG monolayer.

to adopt a helical conformation, the binding to micelles strongly modifying the NOE pattern. Under these conditions (Table 4) and similarly to peptide **1**, strong dNN as well as dNN(i, $i + 2$), $d_\alpha N(i, i + 3)$ and $d_{\alpha\beta}(i, i + 3)$ NOEs were detected in the N-terminal part of the peptide (Figure 6) indicating the presence of an α-helical structure. These findings suggest that the peptides adopt an α-helical conformation in their hydrophobic domain (sequence 3 −16 for peptide **2**) when bound to SDS micelles, whereas in both cases the C-terminus remains disordered. Similarly, upon incorporation into DPC micelles the peptides also undergo a random coil to α-helix transition as monitored by CD. Finally, as both headgroups carry different charges, negative and zwitterionic, respectively, these results indicate that the nature of the headgroups has no significant effect on the conformation of the peptides which are incorporated into their respective micelles.

In order to verify that the α-helical structure only concerns the hydrophobic domain, we repeated the above experiments in media containing TFE. For this we first verified by CD that, as usual, TFE indeed induced the formation of an α-helical structure (Table 1) and then determined the amount of TFE required to reach the maximum of α-helix content (Figure 7). As this amount was determined at 30%, most of the NMR experiments were carried out for **1** in the same solvent conditions (Table 5). The finding of NOEs of the same type as in SDS micelles (Figure 8) confirmed the presence of an α-helix extending from residue 2 to 18. Further additions of TFE, up to 70%, did not induce major modifications in the spectrum except for the appearance of additional NOEs, therefore indicating that the helix extended from residue 1 to 20. As to the remainder of the peptide, which includes mainly the NLS sequence, it is nonordered since no NOE characterizing an ordered structure could be detected in this sequence.

Comparison of both the CD and NMR data provided similar estimated amounts of α-helical content, although the values calculated from the NMR data were slightly higher (10%) than that calculated on the basis of the CD spectra. The origin of this small discrepancy most likely arises from the shortness of the α-helix (from 12 to 16 residues or about 3 to 4.5 helical turns) and therefore from the end effects which generally lead to a lowering of ellipticity.

(B) Study in Media Inducing a β-Type Structure. In contrast to the results obtained in the presence of micelles which promote the formation of an α-helix, the interaction of peptides **1** and **2** with phospholipids in vesicular forms generated a conformational behavior which strongly differed from that described just above. By CD, for technical reasons mainly due to the scattering, the investigations were restricted to DOPG. When added to a suspension of DOPG vesicles in a 25 mM NaCl medium, the peptide underwent a conformational transition characterized by strong modifications in the CD spectrum (Figure 2). In the absence of lipids the CD spectrum showed a single minimum at 198 nm, typical of a nonordered structure. In the presence of lipid, the spectrum was characterized by a single minimum at 218 nm and a maximum at 195 nm. This suggests that upon binding to DOPG vesicles the peptide adopts mainly a β-sheet structure (Table 1). However, the low intensity of this band indicates that we are not dealing with a single conformational state but rather with a mixture or an equilibrium between several conformations where β-sheet structures are the major components.

Since the CD investigations were restricted to only one lipid species and in order to extend the behavior described

above to other lipids, the nature of the polar headgroups of which varied, we investigated the conformations of the peptides in lipid environments by FTIR *(27)*. This technique has the advantage of being applicable to transferred monolayers (Langmuir-Blodgett films) based on a larger variety of lipids such as DOPG and DOPC used in the present work and is sensitive to the identification of β-sheet structures. The infrared spectrum of a transferred monolayer made of pure peptide (Figure 9) indicated the coexistence of several conformational states including β-sheet, α-helix, and random coil, identified by amide I band components at 1620 and 1630 on the one hand and on the other hand 1652 and 1665 cm^{-1} *(28−31)*. The presence of lipid in the monolayer enhanced the amount of β-sheet form, as characterized by a single absorption band. Indeed, as shown in Figure 9, a typical spectrum obtained with DOPG and with DOPC at a lipid/peptide ratio (R_i) of 1 reveals a major amide I contribution lying at 1628 cm^{-1}. It should be noted that the overall spectrum features remain identical upon increasing R_i up to 2 and that they do not depend on the nature of the polar headgroup of the lipid.

All the above data favor the idea that the peptides preferentially adopt a β-sheet conformation when interacting with lipids. However, the positioning of the peptides with respect to the lipids still remains to be identified. For this purpose, two different approaches were initiated; in the first one, we used the fluorescence properties provided by presence of either a single Trp residue in position 18 or by a coumarin fluorophore at the N-terminus of peptide, **1** and in the second, we initiated a study of monolayers containing both lipids and peptide **1**.

Addition of **1** to DOPC or DOPG vesicles generated a blue shift from 352 to 342 nm of the maximum of the emission spectrum accompanied by a slight increase in the fluorescence intensity (about 25%) (Figure 10A). Although, this shift was small (10 nm) compared to that found for a Trp residue going from a polar to a nonpolar environment (30 nm) *(37)*, i.e., from water to a lipid bilayer core, this observation indicated that upon binding to phospholipid vesicles the environment of the Trp^{18} residue became less polar. Although no modification of Trp fluorescence could be detected upon modification of the experimental conditions (pH, concentration), it can be stated that the Trp residue interacts at least superficially with the bilayer surface, but that modification of the Trp environment was due to any conformational change cannot be ruled out. Moreover, since the Trp fluorescence did not provide any information concerning the position of the hydrophobic N-terminus with respect to the lipid bilayer, coumarin labeled peptide was used as probe. The variation of fluorescence of coumarin as a function of lipid/peptide ratio is shown in Figure 10B and reveals a blue shift (7 nm) upon increasing R_i. This shift is similar to that of coumarin when removed from water to cyclohexane, the latter having a dielectric constant almost identical to that of the membrane core *(33)* and therefore suggesting that the coumarin fluorophore is membrane associated.

It should be noted that there is an apparent discrepancy between the amounts of lipid required to induce the β-formation according to the method used for its identification. However, it is worthwhile recalling that FTIR spectra were recorded on transferred monolayers and not on the bulk and, in addition, that the monolayers were obtained by spreading a lipid−peptide mixture on the water surface thus forcing the peptide to be membrane associated. As for the difference which appears when comparing the Trp and coumarin fluorophores, it may be explained by the modification of the peptide properties induced by the linkage to the fluorophore. Indeed, it has previously been shown that the final cellular localization of a coumarin labeled primary amphipathic peptide differs from that of the nonlabeled one *(15)*, indicating changes in the affinity of the peptide for the membrane most likely arising from a modification in the hydrophilic-hydrophobic balance. Therefore, the main information arising from this study must be restricted to a qualitative behavior while a quantitative analysis would require a better knowledge of the peptide properties especially with respect to the water−lipid partitions.

The second approach used for the study of the lipid−peptide interactions was more specifically related to the identification of their nature by measuring binding to monolayers or insertion properties of the peptides. Both peptides were shown to be strongly surface active since they decreased the surface tension of the air/water interface by 25 mN/m at 1 μM peptide concentration (Figure 11A). Insertion experiments were achieved by the same procedure as reported by Rafalski *et al. (34)* by injection of the peptide into the subphase of a phospholipid monolayer, the starting monolayer pressure being slightly lower than that of the peptide at saturation. Figure 11A shows the relative variations in surface tension for a constant surface area when increasing the concentration of peptide **1** in the subphase. For the two lipids used in these experiments, DOPC and DOPG, the peptides increased the surface pressure of the monolayers with similar amplitude (≈16 mN/m). This indicates that the monolayer insertion of the peptides does not or nearly does not depend on the nature of the phospholipid headgroups (negatively charged or neutral) but, however, exhibits slightly higher affinity for DOPG and that strong hydrophobic interactions can still occur. In addition, since the peptides can penetrate the phospholipid monolayer at very high pressures (close to the lipid collapse pressure) (Figure 11B), it is very probable that the hydrophobic interactions arise from direct contacts between the lipidic acyl chains and the hydrophobic domains of the peptides *(35)*.

DISCUSSION

In this work it was shown that peptides generated through association of a signal peptide with a nuclear localization sequence could enter intracellular domains very rapidly. In order to elucidate the mechanism(s) leading to this internalization, we performed a conformational study of these peptides. Owing to the presence of the NLS sequence, the solubility of the signal sequence in water has been strongly improved, therefore enabling most conformational investigations to be carried out in water. CD, FTIR, and NMR measurements revealed that the peptides were random coil in water while they showed a tendency to adopt an α-helical structure in the presence of TFE or of SDS micelles. In both of these latter cases, the CD spectra were characterized by a positive band at 193 nm accompanied by two negative ones at 207 and 222 nm typical of a high α-helical content. From examination of the NOE pattern it appears that the helix covers the hydrophobic core of the peptides and, owing to the line broadening observed for the hydrophobic residues upon binding to the micelles, we concluded that the hydrophobic domain was most likely embedded in the core

of micelles while the NLS sequence at the C-terminus, which is nonstructured, remained located in the water.

When these two peptides are in the presence of phospholipids, the situation is more puzzling and in apparent disagreement with previous observations made by Cornell *et al. (36)* on signal peptides. Indeed, these authors reported that signal peptides tend to adopt an α-helical structure when embedded in lipid-containing media and that this helix is disposed perpendicular to the plane of the lipid. When injected into the subphase of a lipid monolayer at a high initial pressure, it does not penetrate the monolayer and adopts a β-sheet structure *(36)*. In our case, we have shown that the peptides can insert into lipid monolayers in the β-form.

The finding of either an α-helical or a β-sheet like structure upon interaction of the peptides with micelles or lipidic structures, respectively, emphasizes the strong conformational versatility of these peptides. The various factors which govern the formation of one or the other type of structure remain to be identified precisely. However, the nature of the charges of the polar headgroups does not appear to be of major importance since both micellar SDS (negatively charged) and DPC (zwitterionic; i.e., neutral) promote the same α-helical structure while negatively charged (DOPG) and neutral (DOPC) phospholipids promote β-sheet formation.

Finally, from the results described in this paper, we would like to comment on the role of the NLS moiety. Although this sequence does not appear to play a major structural role for the micelle-bound form, this NLS sequence appears, probably through its water solubility, to govern various conformational states.

In conclusion, the present conformational study which deals with peptides containing both a signal peptide sequence and a NLS shows that this type of peptide can adopt various conformational states depending on the nature of their environment. In water, the peptides are disordered; in SDS micelles, they are mainly α-helical, and the helix covers the hydrophobic part while the hydrophilic moiety remains nonordered and they adopt mainly a β-type structure when in a lipid medium. As to the elucidation of the mechanism, which leads to the cellular internalization of the peptides and which was at the origin of the work, the fact that the major lipid-associated structure is that of an antiparallel β-sheet suggests that this structure is responsible for the transmembrane translocation process.

ACKNOWLEDGMENT

Our thanks are due to M. C. Morris for correction of English.

REFERENCES

1. Leonetti, J. P., Mechti, N., Degols, G., Gagnor, C., and Lebleu, B. (1991*) Proc. Natl. Acad. Sci. U.S.A. 88*, 2702−2706.
2. Zelphati, O., Zon, G., and Leserman, L. (1993) *Antisense Res. Dev. 3*, 323−338.
3. Murata, M., Takahashi, S., Kagiwada, S., Suzuki, A., and Ohnishi, S. (1992) *Biochemistry 31*, 1986−1992.
4. Reed, M. W., Fraga, D., Schwartz, D. E., Scholler, J., and Hinrichsen, R. D. (1995) *Bioconjugate Chem. 6*, 101−108.
5. Leonetti, J. P., Degols, G., and Lebleu, B. (1990) *Bioconjugate Chem. 1*, 149−153.
6. Derossi, D., Calvet, S., Trembleau, A., Brunissen, A., Chassaing, G., and Prochiantz, A. (1996) *J. Biol. Chem. 271*, 18188−18193.
7. Brugidou, J., Legrand, Ch., Méry, J., and Rabié, A. (1995) *Biochim. Biophys. Res. Commun. 214*, 685−693.
8. Briggs, M. S., and Gierasch, L. M. (1986*) Adv. Protein Chem. 38*, 109−180.
9. Kalderon, D., Richardson, W. D., Markham, A. F., and Smith, A. E. (1984) *Nature (London) 311*, 33−38.
10. Kalderon, D., Roberts, B. L., Richardson, W. D., and Smith, A. E. (1984) *Cell 39*, 499−509.
11. Goldfarb, D. S., Gariépy, J., Schoolnik, G., and Kornberg, R. D. (1986) *Nature (London) 322*, 641−644.
12. Chaloin, L., Méry, J. Lamb, N., Heitz, A., Bennes, R., and Heitz, F. (1996) in *Peptides. Chemistry, Structure and Biology*, Kaumaya, P. T. P., and Hodges, R. S., Eds., Mayflower Sci. Ltd., pp 501−502.
13. Méry, J., Brugidou, J., and Derancourt, J. (1992) *Pept. Res. 5*, 233−240.
14. Méry, J., Granier, C., Juin, M., and Brugidou, J. (1993) *Int. J. Peptide Protein Res. 42*, 44−52.
15. Vidal, P., Chaloin, L., Méry, J., Lamb, N., Lautredou, N., Bennes, R., and Heitz, F. (1996*) J. Pept. Sci. 2*, 125−133.
16. Girard, F., Fernandez, A., and Lamb, N. (1995) *J. Cell. Sci. 108*, 2599−2608.
17. Girard, F., Strausfeld, U., Fernandez, A., and Lamb, N. 1(991) *Cell 67*, 1169−1179.
18. Wüthrich, K. (1986) *NMR of Proteins and Nucleic Acids*, John Wiley and Sons Inc., New York.
19. Rizo, J., Blanco, F. J., Kobe, B., Bruch, M. D., and Gierasch, L. M. (1993*) Biochemistry 32*, 4881−4894.
20. Chupin, V., Killian, J. A., Breg, J., de Jongh, H. H. J., Boelens, R., Kaptein, R., and de Kruijff, B. (1995) *Biochemistry 34*, 11617−11624.
21. Derossi, D., Joliot, A. H., Chassaing, G., and Prochiantz, A. (1994) *J. Biol. Chem. 269*, 10444−10450.
22. Greenfield, N., and Fasman, G. D. (1969) *Biochemistry 8*, 4108−4116.
23. Batenburg, A. M., Brasseur, R., Ruysschaert, J. M., Van Scharrenburg, G. J. M., Slotboom, A. J., Demel, R. A., and de Kruijff, B. (1988) *J. Biol. Chem. 265*, 8164−8169.
24. Yamamoto, Y., Ohkubo, T., Kohara, A., Tanaka T., Tanaka, T., and Kikuchi, M. (1990) *Biochemistry 29*, 8998−9006.
25. Hoyt, D. W., and Gierasch, L. M. (1991) *Biochemistry 30*, 10155−10163.
26. Rozek, A., Buchhko, G. W., and Cushley, R. J. (1995) *Biochemistry 34*, 7401−7408.
27. Briggs, M. S., Cornell, D. G., Dluhy, R. A., and Gierasch, L. M. (1986) *Science 233*, 206−208.
28. Dong, A., Huang, P., and Caughey, W. S. (1990) *Biochemistry 29*, 3303−3308.
29. Surewicz, W. K., Mantsch, H. H., and Chapman, D. (1993) *Biochemistry 32*, 389−394.
30. Jackson, M., and Mantsch, H. H. (1995) *Crit. Rev. Biochem. Mol. Biol. 30*, 95−120.
31. Rodriguez-Crespo, I., Gomez-Gutierrez, J., Encinar, J. A., Gonzalez-Ros, J. M., Albar, J. P., Peterson, D. L., and Gavilanes, F. (1996) *Eur. J. Biochem. 242*, 243−248.
32. Lakowicz, J. R. (1983) *Principles of Fluorescence Spectroscopy*, Plenum Press, New York.
33. Goya, S., Takadate, A., Fujino, H., Otagiri, M., and Uekama, K. (1982) *Chem. Pharm. Bull. 30*, 1363−1369.
34. Rafalski, M., Lear, J. D., and DeGrado, W. F. (1990) *Biochemistry 29*, 7917−7922.
35. Verger, R., and Pattus, F. (1982) *Chem. Phys. Lipids 30*, 189−227.
36. Cornell, D. G., Dluhy, R. A., Briggs, M. S., McKnight, J., and Gierasch, L. M. (1989) *Biochemistry 28*, 2789−2797.

BI9708491